Polycyclic Aromatic Hydrocarbons and the Diffuse Interstellar Bands. A Survey

F. Salama

NASA-Ames Research Center, Space Science Division, Mail Stop 245-6, Moffett Field, California 94035-1000, USA

G. A. Galazutdinov

Special Astrophysical Observatory, Nizhnij Arkhyz 357147, Russia

J. Krełowski

Nicolaus Copernicus University, Center for Astronomy, Gagarina 11, Pl-87-100 Toruń, Poland

L. J. Allamandola

NASA-Ames Research Center, Space Science Division, Mail Stop 245-6, Moffett Field, California 94035-1000, USA

and

F.A. Musaev

Special Astrophysical Observatory, Nizhnij Arkhyz 357147, Russia

Received _____; accepted _____

ABSTRACT

We discuss the proposal relating the origin of some of the diffuse interstellar bands (DIBs) to neutral and ionized polycyclic aromatic hydrocarbons (PAHs) present in interstellar clouds. Laboratory spectra of several PAHs, isolated at low temperature in inert gas matrices, are compared with an extensive set of astronomical spectra of reddened, early type stars. From this comparison, it is concluded that PAH ions are good candidates to explain some of the DIBs. Unambiguous assignments are difficult, however, due to the shift in wavelengths and the band broadening induced in the laboratory spectra by the solid matrix. Definitive band assignments and, ultimately, the test of the of the proposal that PAH ions carry some of the DIB must await the availability of gas- phase measurements in the laboratory. The present assessment offers a guideline for future laboratory experiments by allowing the preselection of promising PAH molecules to be studied in jet expansions.

Subject headings: dust, extinction – ISM: abundances – ISM: general

1. Introduction

Interstellar HI clouds are characterized by various absorption features which are superposed on the spectra of early type, reddened, OB stars. These absorption features form several classes:

- The continuous extinction is the selective attenuation of starlight. It is thought to be caused by interstellar dust grains. (for a review see Mathis (1990) or Krełowski & Papaj (1993)).

- The polarization of starlight is caused by the partial alignment of the dust grains with the interstellar magnetic field (for a review see Whittet (1996)).

- Spectral resonant lines due to rarefied atomic gases (most of them fall in the far-UV range; Morton, 1975). The line pattern changes from object to object – *e.g.* Crawford (1989). In the visual wavelength range, the set of lines consists of Fraunhofer D_1 and D_2 of NaI as well as H and K of $CaII$ and the weaker lines of FeI, KI and CaI.

- Absorption features of simple molecular species (CH, CH^+, CN, C_2, NH, H_2, CO), some of them known since the late 1930's. Their intensity-to-E_{B-V} ratios vary strongly from cloud to cloud (Crawford, 1989; Krełowski et al., 1992; Snow, 1992).

- A set of ubiquitous absorption features, the diffuse interstellar bands (DIBs), which remains unidentified since its discovery by Heger in 1922. The DIB spectrum consists of more than two hundred confirmed interstellar bands including a large number of weak features. For a recent review, see Herbig (1995).

Here, we focus on the DIBs and, more specifically, on the potential link between the polycyclic aromatic hydrocarbon (PAH) ions and the carriers of the bands.

The PAH-DIB proposal has been put forward, more than a decade ago, on the basis of the expected abundance of PAHs in the interstellar medium and their stability against UV photodissociation (Van der Zwet & Allamandola, 1985; Léger & d'Hendecourt, 1985; Crawford et al., 1985). PAHs are now thought to be largely responsible for the discrete infrared emission bands observed at 3.3, 6.2, 7.7, 8.6 and 11.3 μm in many astronomical objects including HII regions, planetary and reflection nebulae, and the ISM of the Milky Way and other galaxies. Recent observations from the IR space satellites ISO (Mattila et al., 1996) and IRTS (Onaka et al., 1996) have confirmed that PAHs are ubiquitous throughout the general diffuse ISM as well. According to the astrophysical model, PAHs are expected to be present as a mixture of free, neutral and ionized, molecules following a large size distribution which range from small, gas-phase, molecules ($\leq$ 25 carbon atoms) to large graphitic platelets (Allamandola et al., 1989; Puget & Léger, 1989). PAHs are considered to form a link between the gas and the solid phase of interstellar dust and to be a key element for the coupling of stellar FUV photons with the interstellar gas.

Initial testing of the PAH-DIB proposal was hampered by the lack of laboratory spectra of PAHs taken under astrophysically relevant conditions. This situation has, however, improved thanks to the laboratory studies that have been performed to measure the spectroscopic properties of neutral and ionized PAHs in astrophysically relevant media, i.e., PAHs truly isolated at low temperature (4.2 K) in neon matrices (Salama & Allamandola, 1991, 1992a, 1992b, 1993; Salama, Joblin & Allamandola, 1994, 1995; Ehrenfreund et al., 1992, 1995; Léger, d'Hendecourt, & Défourneau, 1995). Based on these data and on the astronomical data then available, the PAH-DIB proposal has been re-assessed (Salama 1996, Salama et al., 1996, Salama, Joblin & Allamandola, 1995) with the conclusion that PAH ions were indeed very promising candidates for the DIB carriers. Since then, the laboratory and astronomical data sets have both considerably evolved in size. An extensive set of matrix- isolated spectra of PAH ions is now available

(Salama, 1996, Salama et al., 1999). Very recent, follow-up, experiments (Romanini et al., 1999; Bréchignac & Pino, 1999) have now opened the way for a similarly extensive study in the gas phase. Here, we compare the extensive set of laboratory spectra available for about 15 PAH ions isolated in neon matrices to an extensive set of high-resolution astronomical data. The objectives are (i) to confirm the correlations previously found between some specific PAH ions and some specific DIBs (Salama, Joblin & Allamandola, 1995, Salama, 1996) against higher-resolution astronomical data, (ii) to search for new DIBs at the positions predicted by laboratory measurements, (iii) present a set of potential PAH candidates for studies in the gas phase and, (iv) to further assess and test the validity of the PAH-DIB proposal.

In section 2, we briefly review the current state of knowledge regarding the DIBs. This is followed, in section 3 and 4, by a description of the astronomical and laboratory data sets, respectively. In section 5, we discuss the results of this assessment.

2. Diffuse interstellar bands

The diffuse interstellar bands are absorption features superposed on the interstellar extinction curve. They fall in the near-ultraviolet to the near-infrared range (4400 - 10,000 Å). The bands are characterized as diffuse due to the observation that they are broad and shallow in comparison to the well-known, narrow, interstellar atomic lines. The individual DIBs vary widely in strength and shape, with equivalent width per magnitude of visual extinction ranging from about 2 Å to the detection limit of about 0.006 Å. The full width at half maximum (FWHM) values for the DIBs range from about 0.4 to 40 Å.

The features centered around 5780 and 5797 Å were the first DIBs to be recognized as "stationary" lines in the spectra of spectroscopic binaries (Heger, 1922). Their interstellar

nature was established by Merrill (1934, 1936), and Beals & Blanchet (1937). The survey of Herbig (1975) reported 39 DIBs. Since that time the number of DIBs has been extended to more than 220 (Herbig, 1988; Herbig & Leka, 1991; Jenniskens & Désert, 1994 and Krełowski, Sneden & Hiltgen, 1995). The most recently discovered DIBs are very weak with typical equivalent width per magnitude of visual extinction of the order of 0.01 Å.

Despite intense efforts, no definitive identification of the carrier(s) of the DIBs has been made. Various candidates have been proposed as possible carriers for the bands, ranging from impurity-doped dust grains, to free, neutral and ionized, molecular species of varying sizes and structures (Tielens & Snow, 1995), to molecular hydrogen (Sorokin and Glownia, 1995). It is now clear that the DIBs cannot be explained by the early concept of a single carrier due to the large number of bands detected and the lack of correlation between the bands. It is now thought that *(i)* the carriers are large, carbon-bearing, gas-phase molecules in either the neutral and/or ionized forms and *(ii)* these molecular carriers are part of an extended size distribution of the interstellar dust (Tielens & Snow, 1995). Structure within the profiles of a few strong DIBs is now seen in high-resolution observations. This structure is generally interpreted as the signature of the rotational band structure of gas-phase molecules (Ehrenfreund and Foing, 1996; Jenniskens et al., 1996; Kerr et al., 1998). Quite recently, laboratory experiments on the gas-phase spectroscopy of various C-chains have shown a very good match between the positions and relative intensities of bands of C_7^- and 6 DIBs (Tulej et al., 1998). This results supports an origin of the DIBs in C-rich molecules.

The problem of the identification of the DIB carriers is further complicated by the fact that many DIBs overlap (Herbig, 1975). For example, the prominent 5780 DIB (henceforth, the major bands will be labeled by their approximate central wavelengths in Å) overlaps with the very broad ($\simeq$ 20 Å) but extremely shallow 5778 DIB. Further structure within the

general profile of this broad band has been suggested by Herbig (1975) and demonstrated by Krełowski, Schmidt & Snow (1997). The latter paper also shows that the weak features are of a different origin and thus they are simply blended with the 5778 DIB.

The Doppler splitting of the sharp profiles of interstellar atomic lines also affects the DIB profiles. Herbig & Soderblom (1982) have shown that the very narrow 6196 DIB has a complex, Doppler–split profile along some lines-of-sight. It is now clear that the DIBs observed in the spectra of heavily reddened, distant, stars are composed of multiple components each originating in individual clouds of different radial velocities and different physical properties. In the case of the broader DIBs, the Doppler splitting is not seen directly, but the resultant profiles are much broader than in single-cloud cases (*e.g.*, Westerlund & Krełowski, 1988). It should be emphasized that when the clouds along any sightline produce different spectra (as shown by Krełowski & Westerlund (1988) or Krełowski & Walker (1987)), the resulting observation is an ill-defined average spectrum of all these clouds and any interpretation of the data becomes very difficult.

Recent observations have demonstrated that all of the well–known DIBs (i.e., the stronger features) are of different origin (Moutou et al., 1999). However, Krełowski, Schmidt & Snow (1997) found that the newly discovered, weak, interstellar features may be related to the strong ones. This implies that the spectrum of any potential DIB carrier consists of a single strong band together with several weak features. Note that this requirement is met by the spectra of PAH ions as discussed below.

It is also important to mention that the study of Moutou et al. (1999) modifies the concept of "families" of diffuse bands initially introduced by by Krełowski & Walker (1987). This latest survey shows that the DIB "families" are sets of features whose carriers co–exist in the same clouds, i.e., under the same physical conditions. This doesn't necessarily imply that the bands belonging to one "family" share a common origin.

3. The observational program

The survey, described below, is based on three new sets of observational data. Heavily reddened stars have been selected to facilitate the detection of weak spectral features. In many cases the same object has been observed with more than one instrument to compare data from different sources and to ensure that the weak features traced in the spectra are real and that their intensities can be measured with a reasonable accuracy.

Most of the spectra discussed here have been acquired with the two, very similar, echelle spectrometers which allow coverage of the wavelength range from ~3500 Å to ~10,100 Å in one exposure with a resolution of 45,000 as described by Musaev (1993). The spectrometers are fed either with the 1m Zeiss telescope of the Special Astrophysical Observatory (SAO) of the Russian Academy of Sciences or with the 2 m telescope of the Observatory on top of the Terskol peak (Northern Caucasus). The spectrometers are equipped with 1242x1152 CCDs (Wright Instruments; pixel size 22.5μm x 22.5μm) and can acquire spectra of stars as faint as ~9 mag.

The echelle spectra were reduced using the DECH code described by Galazutdinov (1992). This program allows flatfield division, bias/background subtraction, one–dimensional spectrum extraction from the 2–dimensional images, diffuse light correction, spectrum addition, removal of cosmic ray features, etc. The DECH code also allows the location of continuum levels, the measurement of line equivalent widths, positions and shifts, etc. The spectral range, covered in every exposure, contains strong and well–identified interstellar atomic lines, CaII, CaI, NaI and KI, for rest–wavelength calibrations.

Some of the spectra have been acquired by one of us (JK) at the McDonald Observatory in Texas. The total set of collected spectra contains data for ~80 objects – OB stars, more or less reddened. All the spectra cover the wavelength range from ~5600Å to

~7000Å with a resolution of 60,000 and have been acquired with the Sandiford echelle spectrograph installed at the Cassegrain focus of the 2.1 m telescope. The data acquisition and reduction techniques are described in Krełowski & Sneden (1993). The set of the McDonald spectra contains data for many reddened objects as well as for a few objects considered as unreddened standards which are in fact very slightly reddened and which are also considered in this survey. The set of McDonald spectra is characterized by an exceptionally high S/N ratio from 500 to 1000.

Table 1 lists the objects considered in this paper together with their spectral types, luminosity classes, color excesses, and the apparent rotational velocities. Weak interstellar features, observed in spectra of rapidly rotating stars (HD210839) cannot be of stellar origin. The observed colors have been taken from the SIMBAD database and the intrinsic colors from the paper of Papaj, Krełowski and Wegner (1993). We have selected heavily reddened stars to enhance the detection of weak interstellar features. We have also selected stars which are characterized by different strength ratios for the major DIBs 5780 and 5797 because it has been shown (Krełowski, Sneden & Hiltgen, 1995) that the pattern of the weak features varies with the ratio of the strength of the 5780 and 5797 DIBs.

EDITOR: PLACE TABLE 1 HERE.

4. The Laboratory program

Matrix isolation spectroscopy (MIS) is used to simulate in the laboratory environmental conditions which are close to the conditions known (or expected) in the diffuse interstellar medium. In MIS experiments, the neutral and ionized PAHs are fully isolated at low temperature (< 5 K) in the low-polarizability neon matrices where the perturbations induced in the spectrum of the trapped molecules/ions are minimum. Until PAHs can be

Table 1. Basic stellar data

HD or BD	Sp/L	V	B-V	E(B–V)	v×sin(i)	Observatory
183143	B7Ia	6.84	1.27	1.28	60	Terskol, McDonald
186745	B8Ia	7.00	+0.93	1.00	126	Terskol
187459	B0.5I	6.40	0.20	0.41	126	SAO
190603	B1.5Iae	5.64	0.56	0.73	32	SAO
194279	B1.5Ia	7.01	1.03	1.20	50	Terskol
195592	O9.5Ia	7.10	0.87	1.11	300	SAO
207198	O9IIe	5.95	0.31	0.54	76	Terskol
210839	O6 Iab	5.06	+0.23	0.52	285	McDonald
224055	B3Ia	7.17	0.70	0.83	45	Terskol
BD+40 4220	O7e	9.10	1.67	1.96	>400	Terskol

routinely studied in supersonic jets, MIS remains the best tool available to simulate the conditions of the diffuse ISM (Salama, 1996).

The experimental apparatus and protocol have been described elsewhere (Salama and Allamandola, 1991; Salama, Joblin & Allamandola, 1994) and only a synopsis is given here. Briefly, the experimental apparatus consists of a cryogenic sample chamber which is part of a high-vacuum system and consists of 4 ports at 90^0 and two gas injection ports at 45^0. The sample holder suspended at the center of the chamber is cooled down to 4.2 K by a liquid He transfer cryostat. The substrate (sapphire) can be positioned to face alternatively the spectroscopy ports, the gas injection ports, an irradiation lamp, or vacuum deposition furnace. The spectral light sources consist of a 160-360 nm output D_2 lamp and a 320-2500 nm output tungsten filament lamp. The light collected at the spectroscopy port of the sample chamber is guided to the entrance slit of a triple grating monochromator by a fiber optic cable and detected by a CCD array mounted directly on the exit port and interfaced to the computer system. The ionization source is a microwave-powered, flow discharge hydrogen lamp generating photons of 10.2 eV energy (Lyman α line). The PAH sample is simultaneously condensed with the neon gas onto the cold substrate. The frozen matrix is then spectroscopically analyzed. Ions are generated *in situ* from the stable precursor, via vacuum- ultraviolet (VUV) photoionization.

VUV irradiation of the neutral PAHs isolated in Ne matrices produces *new spectral features* in the UV-NIR range (1800-10,600 nm). The new features are found to be associated with the PAH cation (PAH^+) formed by direct, one-photon, ionization of the neutral precursor. Some representative spectra are shown in Figures 1 and 2 for the PAH cations phenanthrene ($C_{14}H_{10}^+$), benzo(e)pyrene ($C_{20}H_{12}^+$), benzo(ghi)perylene ($C_{22}H_{12}^+$) and pentacene ($C_{22}H_{14}^+$).

EDITOR: PLACE FIGURE 1 HERE.

EDITOR: PLACE FIGURE 2 HERE.

The astrophysical implications derived for small PAH ions ($\leq$ 10 rings, i.e., $\leq$ 25 C-atoms) have been discussed in the literature (Salama et al., 1996, Salama, 1996) and are recapitulated below:

(i) Contrary to their neutral precursors, *ionized PAHs absorb in the visible and NIR and could contribute to the DIBs* (see Figures 1 and 2). Large PAH ions ($\geq$ 100 rings, i.e., containing more than 250-300 C-atoms) are not expected, however, to contribute significantly to the DIBs.

(ii) The NUV-to-NIR absorption spectrum of PAH cations is dominated by a single band. This is the spectral range of interest for comparison with the DIBs. The stronger PAH ion transitions measured in Ne are compared in Table 2 with the known DIBs. The fractional shift in energy is well within the 0.5% shift generally expected between Ne matrix and gas phase measurements (Bondybey & Miller, 1983; Salama, 1996; Romanini et al., 1999).

(iii) In the case of compact PAHs (such as $C_{16}H_{10}^{+}$ and $C_{22}H_{12}^{+}$ shown in Figure 1), the strongest absorption lies at the high energy end of the spectrum and its oscillator strength is of the order of 0.1. In the case of non-compact PAHs (such as $C_{10}H_{8}^{+}$, $C_{14}H_{10}^{+}$ and $C_{22}H_{14}^{+}$ shown in Figure 2), the strongest absorption lies at the low energy end of the spectrum and has an oscillator strength in the range 0.001-0.1.

5. Comparison of astronomical spectra with laboratory spectra

Figures 3 - 7 show the spectra of heavily reddened stars in the vicinity of the major PAH ion features measured in laboratory experiments. Features were searched for in 100 Angstrom windows around laboratory peak wavelength positions. This criterium for the

wavelength width has been chosen to take into account the upper limit to the wavelength shift known to be induced by the solid matrix (Salama 1996). In all the figures, the interstellar spectral features are plotted in the laboratory wavelength scale for the gas phase lines. Such features are very abundant, especially in the near–IR. As shown in section 4 above and in Figures 1 and 2, the PAH ion candidates produce one strong band together with several weaker features in the NUV-to-NIR range.

EDITOR: PLACE FIGURE 3 HERE.

EDITOR: PLACE FIGURE 4 HERE.

EDITOR: PLACE FIGURE 5 HERE.

EDITOR: PLACE FIGURE 6 HERE.

EDITOR: PLACE FIGURE 7 HERE.

Table 2 compares the PAH features, measured in the laboratory, with their possible astronomical counterparts. Here, the window for comparison has been chosen such as to cover a fractional shift of 0.5% in energy for the laboratory measured absorption bands (Salama 1996). This value is a conservative estimate (and an upper limit) based on the very limited gas-phase data set that is available for comparison. The shift in band positions induced by a Ne matrix is expected to be small. For example, a gas-phase-to-Ne fractional shift of 0.3 – 0.5% is measured for $C_6F_6^+$ and its derivatives (Bondybey & Miller 1983) and a value of 0.5% has been recently derived in the case of $C_{10}H_8^+$ (Romanini et al., 1999).

6. Discussion

DIBs can be roughly classified as strong (band equivalent widths, W_λ, $\geq$ 1.0 Å), moderately strong (1.0 Å$\geq W_\lambda \geq$ 0.1 Å), and weak ($W_\lambda \leq$ 0.1 Å) (Salama et al. 1996). There are only 3 strong DIBs and less than 50 moderately strong DIBs tabulated in Herbig (1995) towards the star HD 183143. All the rest of the DIBs (i.e., the vast majority) range from weak to very weak (less than 0.01 Å equivalent widths). The recent, high quality, spectra of reddened stars makes it possible to reliably detect hundreds of weak interstellar features. All the weak features exhibit the same characteristics as the well–known, stronger, DIBs (Ehrenfreund and Foing 1996, Jenniskens et al. 1996, Kerr et al. 1998) and are also most likely of molecular origin. These features are observed in practically all environments, including the very diffuse clouds (Galazutdinov et al. 1998a). This indicates that the (molecular) carriers of the weak DIBs must be resistant against the UV photon background. Although the increased number of observed features provides more clues for the identification of the band carriers, unambiguous assignments are now more complex. Another difficulty comes from the fact that the weak interstellar features are most densely distributed in the near–infrared spectral range. This range is also populated with numerous telluric lines, mostly due to water vapor which often mask the presence of potential interstellar bands (Galazutdinov et al. 1998b). Only in the cases of a very dry atmosphere can the removal of telluric lines be complete.

As illustrated in Figures 1 and 2, the spectrum of a PAH cation in the NUV-to-NIR spectral range is characterized by a single, strong feature and several related weak bands (i.e. weaker by, at least, an order of magnitude). The weaker bands associated with a specific PAH ion are expected to be observed only when the strongest PAH feature is associated with one of the strong or moderately strong, well–known, DIBs. Inversely, if the strongest feature of a PAH ion corresponds to one of the weak DIBs observed in our spectra

(i.e., the features observed at the level of detection, see Figs. 3-7) there is, obviously, no possibility of detecting the weaker PAH band relatives which would be no deeper than 0.001 of the continuum. In other words, there are two scenarii which can be met while attempting to identify specific DIBs with specific PAH ions: (i) a situation where many absorption bands of a single PAH ion correlate with a combination of strong and weak DIBs. This is the most rewarding situation where a decisive and unambiguous spectral identification can be made based on the comparison of the wavelength positions, energy intervals and relative intensities of numerous bands, (ii) a situation where the strongest absorption band of a PAH ion correlates with a weak DIB. This in itself does not represent a spectral fit. The assignment gains credibility, however, if a significant number of PAH ions (10 or more) are found to be correlated with weak DIBs. Examining now the laboratory (MIS) spectra of PAH ions against these two criteria it becomes possible to identify a number of PAH ions which could be potential DIB carriers. Of course, because of the small neon matrix-to-gas phase shift, the selected PAH ions must then be studied in the gas phase in jet expansions to provide the test for a decisive comparison in wavelengths and band profiles with the astronomical spectra.

Table 2 shows the comparison between the laboratory data for 14 PAH ions and the astronomical bands measured in the spectra of 5 of the reddened objects listed in Table 1. The window for comparison has been chosen such as to encompass a possible fractional shift of 0.5% in energy for the laboratory MIS absorption bands as compared to the gas phase. This window encompass, thus, any expected shift induced by the solid neon matrix (see the discussion above). Following this criterium and despite the fact that the weak DIB features are quite abundant in the NIR, it is found that, with the exception of the 7580 Å band of the 1-methylpyrene ion, each specific laboratory band is correlated to no more than 3 DIBs in most cases (i.e., no more than 3 DIBs are found in any "error box" centered on the laboratory band position). Table 2 also indicates that about a third of the elements in

the laboratory database (5 PAH ions out of 14) exhibit a potential correlation with DIBs. Four other PAH cations have their strongest transitions in the range $8800 - 9400\AA$ which is heavily obscured by telluric water vapor bands. Moreover, out of the 24 DIBs which are found to fall in the wavelength windows, 5 can be described as strong to moderately strong while the rest of the bands range from weak to very weak. This comparison leads to the following conclusions:

1- Among the 5 PAH ions which show a clear positive correlation with DIBs, 3 PAHs -1-methylpyrene, carbohydroxypyrene and tetracene- correlate with strong to moderately strong DIBs. The 2 other PAHs, benzo(ghi)perylene and naphthalene, are correlated with very weak DIBs.

2- Among the 9 PAH ions which are not detected, coronene, perylene, pyrene, and its derivative 4-methylpyrene can be ruled out and are not expected to significantly contribute to the DIBs because their strongest absorption is not detected in the astronomical spectra. Note that a previous search for the coronene and ovalene ions in the spectra of 5 reddened stars (including BD +40 4220) had also yielded a negative result (Ehrenfreund et al. 1995). The strongest transition of benzo(e)pyrene is blended with the interstellar CaI $4227\AA$ band (Table 2). The case of phenanthrene and its derivative 1-methylphenanthrene, benzanthracene and pentacene is less clear because their strongest transitions fall (Figure 2) in a region heavily obscured by telluric lines. We note, however, that for both the phenanthrene and pentacene ions, a DIB is observed near the position of the second strongest band of the spectrum in each case. We discuss, below, each case of positive correlation.

6.1. $1-methylpyrene^+$

The absorption spectrum of the photolysis product of 1-methylpyrene ($(CH_3)C_{16}H_9$) is dominated by a band at 4442 Å which falls close to the strong 4429 DIB (0.3% shift). This band has been tentatively assigned to the methylene- pyrene cation. The other very strong band seen in the laboratory spectrum has been shown to belong to a different photolysis product of methylpyrene (Léger, d'Hendecourt, & Défourneau, 1995). The weaker 7580 Å band can be correlated to more than one weak DIB in the range 7558 to 7585 Å (see Table 2).

6.2. $Carbohydroxypyrene^+$

The absorption spectrum of the photolysis products of carbohydroxypyrene ($(COH)C_{16}H_9$) is dominated by a band at 4499 Å which falls close to the moderately strong 4502 DIB (0.07% shift). By analogy with the case of methylpyrene, this band is tentatively assigned to the cation $(COH)C_{16}H_9^+$. The other strong band seen in the laboratory spectrum belongs to a different photolysis product of carbohydroxypyrene. The weaker band around 8980 Å falls in the region obscured by telluric lines (Table 2).

6.3. $Tetracene^+$

The absorption spectrum of the tetracene ion ($C_{18}H_{12}^+$) is dominated by a band at 8648 Å which falls close to the very strong 8621 DIB (0.3% shift). This correlation is only tentative because the spectrum shows, in this case, strong band splitting induced by the matrix (Table 2). Moreover, the other moderately strong band of the tetracene ion which falls at 8373 Å has not been detected yet in the astronomical spectra.

6.4. *Naphthalene*$^+$

The case of the naphthalene ion ($C_{10}H_8^+$) has been discussed in detail in a recent paper presenting the first gas-phase spectrum of a PAH ion isolated in an expansion jet (Romanini et al., 1999). One can now directly compare the laboratory spectra to the astronomical spectra. From this preliminary study, it appears that the two strongest bands of $C_{10}H_8^+$ fall at 6706 and 6489 Å and may be associated with the very weak 6699 and 6492 DIBs. The relative intensity of the 2 bands was found to be the same ($\sim$1.8) in the laboratory and in the astronomical observations available at that time (Jenniskens & Désert (1994)). However, our astronomical survey indicates that the relative intensity of these 2 bands is variable (from 1.2 to 5.2) making it unlikely that these 2 bands be of the same origin. This discrepancy between the two astronomical surveys dramatically illustrates the difficulty of accurately measuring the equivalent widths of weak DIBs as noted previously (Salama 1996). Moreover, it is likely that the 6492 DIB is blended with the FeII 6491.7 Å stellar line in the spectra of HD 183143 and HD 21389 reported by Jenniskens and Désert (1994). The 2 DIBs also have similar FWHM (0.6 and 0.8 Å, respectively) which are about 20 times narrower than those associated with the naphthalene ion bands (14 and 18 Å, respectively). Moreover, when applying the fractional shift of 0.5% in energy measured between the gas phase and the neon matrix values to the other strong vibronic band of $C_{10}H_8^+$, a projected position of 6116 Å is found. This value is very close to the weak 6117 Å DIB which has a width of 0.5 Å. If, alternatively, the strongest of $C_{10}H_8^+$ band at 6706 Å is correlated with the very weak 6702 Å DIB, the other vibronic bands of $C_{10}H_8^+$ are not detectable. In conclusion, the case of of $C_{10}H_8^+$ is weak but not yet settled and awaits further laboratory experiments in the gas phase (see Table 2).

6.5. *Benzo(ghi)perylene*$^+$

Finally, in the case of the benzo(ghi)perylene ion, the spectrum is clearly dominated by a band at 5022 Å which falls close to the very weak 5022.4 DIB (0.01% shift). This makes it impossible to detect the much weaker benzo(ghi)perylene band at 7585 Å (see Table 2 and Figure 1).

In conclusion, we reiterate that the direct comparison of the MIS spectra of PAH ions with the spectra of selected reddened stars cannot yield to a decisive, unambiguous, identification of DIB carriers. This is because (i) the spectra measured in the laboratory are subject to band position shifts induced by the solid matrix and (ii) the stellar spectra contain so many interstellar features that only a precise experimental determination of the wavelengths of molecular features *together* with their gas–phase profile can allow a definitive identification. A comparison between the MIS laboratory data and the astronomical observations is useful, however, when the matrix-to-gas-phase shift is taken into account. The MIS data provide, then, an essential guide for the selection of PAH ions to be spectroscopically studied in a jet expansion (i.e., under conditions which mimic the conditions reigning in the interstellar medium) much more challenging experimentally. The MIS data indicate that a substantial number of PAH ions are promising candidates for the DIB carriers. Out of a laboratory set of only 14 PAH ions which sample compact and non- compact PAHs, hydrogenated PAHs, and PAHs with a heteroatom, 5 exhibit a positive correlation with DIBs, 5 cannot be settled, and 4 can be disregarded as potential DIB carriers. The jet experiments which are just now being developed will provide the much needed data to definitively assess the validity of the PAH proposal with regards to the DIBs. More astronomical surveys of DIB objects are also needed, especially in the wavelenght ranges which have not been as yet frequently observed. The spectrograph used in this project is particularly adapted to this task and will be used to collect an extensive

set of high quality spectra of reddened stars.

This work has been supported by the II US–Poland Maria Skłodowska–Curie Joint Fund under the grant MEN/NSF–94–196. GAG acknowledges the support of the Nicolaus Copernicus University in Toruń. GAG and FAM acknowledge the financial support of the Russian Foundation of Basic Research (Grant 98-02-16544). The Laboratory Research covered in this review has been supported by grants from NASA (Office of Space Science, Astrophysics program) to F. S.

REFERENCES

Allamandola, L. J., Tielens, A. G. G. M. and Barker, J. R. 1989, ApJS, 71, 733.

Beals, C.S. and Blanchet, G.H. 1937, PASP, 49, 224.

Bondybey, V. E., and Miller, T. A. 1983, in *Molecular Ions: Spectroscopy, Structure and Chemistry*, eds. T. A. Miller and V. E. Bondybey, (North Holland Publishing Company), p. 138.

Bréchignac, Ph., and Pino, Th. 1999, A&A, submitted.

Crawford, I.A. 1989 MNRAS, 241, 575.

Crawford, M. K., Tielens, A. G. G. M., and Allamandola, L. J. 1985, ApJ, 293, L45

Ehrenfreund, P., d'Hendecourt, L., Verstraete, L., Léger, A., Schmidt, W. and Defourneau, D. 1992, A&A, 259, 257.

Ehrenfreund, P., Foing, B. H., d'Hendecourt, L., Jenniskens, P. and Désert, F. X. 1995 A&A, 299, 213.

Ehrenfreund, P.and Foing, B. H. 1996 A&A, 307, L25.

Galazutdinov, G. A. 1992, Preprints Spets. Astrof. Obs. , No. 92.

Galazutdinov, G. A., Krełowski, J., Moutou, C. and Musaev, F. A. 1998a, MNRAS, 295, 437.

Galazutdinov, G. A., Krełowski, J., Musaev, F. A., Ehrenfreund, P. and Foing, B. H. 1998b, MNRAS, (submitted).

Heger, M.L. 1922, *Lick Obs. Bull.*, 10, 146.

Herbig, G.H. 1975, ApJ, 196, 129.

Herbig, G.H. 1988, ApJ, 331, 999.

Herbig, G., H. and Soderblom, D. R. 1982, ApJ, 252, 610.

Herbig, G. H. 1995, ARA&A, 33, 19.

Herbig, G.H. and Leka, 1991, ApJ, 382, 193.

Jenniskens, P. and Dèsert, X. 1994, A&AS, 160, 39.

Jenniskens, P., Porceddu, I., Benvenuti, P., and Dèsert, X. 1996, A&AS, 313, 649.

Kerr, T. H., Hibbins, R. E., Fossey, S. J., Miles, J. R. and Sarre, P. J. 1998, ApJ, 495, 941.

Krełowski, J. and Walker, G.A.H., 1987, ApJ, 312, 860.

Krełowski, J. and Westerlund, B.E., 1988, A&A, 190, 339.

Krełowski, J., Snow, T.P., Seab, C.G. and Papaj, J. 1992, MNRAS, 258, 693.

Krełowski, J. and Papaj, P. 1993, PASP, 105, 1121.

Krełowski, J. and Sneden, C. 1993, PASP, 105, 1141.

Krełowski, J., Sneden, C. and Hiltgen, D. 1995, *Planetary Space Sci.*, 43, 1195.

Krełowski, J., Schmidt, M. and Snow T.P. 1997, PASP, 109, 1135.

Léger, A., and d'Hendecourt, L. B. 1985, A&A, 146, 81

Léger, A., d'Hendecourt, L. and Defourneau, D. 1995, A&A, 293, 53.

Mathis, J.S. 1990, ARA&A, 28, 37.

Mattila, K et al. 1996, A&A315, L353.

Merrill, P.W. 1934, PASP, 46, 206.

Merrill, P.W. 1936, PASP, 48, 179.

Morton, D.C., 1975 ApJ, 197, 85.

Moutou, C, Krełowski, J. d'Hendecourt, L. and Jamroszczak, J. 1999, A&A(submitted).

Musaev, F.A. 1993, Pišma v AZh, 19, 776.

Onaka, T. et al. 1996, Publ. Astron. Soc. Japan 48, L59.

Papaj, J., Krełowski, J., Wegner, W. 1993, A&A, 273, 575.

Puget, J. L. and Léger, A. 1989, ARA&A, 27, 161.

Romanini, D., Biennier, L., Salama, F., Katchanov, A., Allamandola, L. J., Stoeckel, F. 1999, Chem. Phys. Lett., submitted.

Salama, F., and Allamandola, L.J. 1991. J. Chem. Phys., 94, 6964

Salama, F., and Allamandola, L.J. 1992a. ApJ, 395, 301.

Salama, F., and Allamandola, L.J. 1992b. Nature 358, 42.

Salama, F., and Allamandola, L.J. 1993. J. Chem. Soc. Faraday Trans. 89, 2277.

Salama, F., Joblin, C., and Allamandola, L.J. 1994. J. Chem. Phys., 101, 10252

Salama, F., Joblin, C., and Allamandola, L.J. 1995. Planet. Space Sci. 43, 1165

Salama, F., Bakes, E. L. O., Allamandola, L. J. and Tielens, A. G. G. M. 1996 ApJ, 458, 621.

Salama, F. 1996. In *Low Temperature Molecular Spectroscopy*, R. Fausto ed., Kluwer, 483, 169.

Salama, F., Joblin, C., and Allamandola, L.J. 1999. in preparation.

Snow, T. P., 1992, *Australian J. Phys.*, **45**, 543.

Sorokin, P. P. and Glownia, J. H. 1995, *Chem. Phys. Letters*, **234**, 1.

Tielens, A. G. G. M. and Snow, T. P. (eds) 1995, *The Diffuse Interstellar Bands, IAU Coll. 137*, Kluwer, Dordrecht.

Tulej, M., Kirkwood, D.A., Pachkov, M., and Maier J. 1998, ApJ, 506, L69.

Van der Zwet, G. P., and Allamandola, L. J. 1985, A&A, 146, 76

Westerlund, B., E. and Krełowski, J. 1988, A&A, 203, 134.

Whittet, D.C.B., 1996 in *Polarimetry of the Interstellar Medium*, W.G. Roberge and D.C.B. Whittet (eds.) ASP Conf. Ser. Vol. 97, p. 125.

This manuscript was prepared with the AAS LaTeX macros v4.0.

λ PAH⁺ (Ne matrix data)	HD207198 Sp=O9 Iie E(B-V)=.60	BD +40 4220 Sp=O7e E(B-V)=1.96	HD 195592 Sp=O9.5Ia E(B-V)=1.14	HD 190603 Sp=B1.5Iae E(B-V)=0.72	HD 187459 Sp=B0.5I E(B-V)=.41
3442 TetracB					
4227 B(e)pyrA	Blended with interstellar CaI (4226.734), 9.5% 18mA				
4395 PyreneA				Intersellar CaI 4226.73, 5.5%, 4mA	Interstellar CaI 4226.73, 10mA
4442 1MePyrA	DIB 4428.88, 6.5%, 450mA				
4456 4MePyrA				DIB 4428.88, 4.5%, 400mA	DIB 4428.88, 3%, 200mA
4499 COHPyrA	DIB4501.8, 4%, 140mA				
4580 4MePyrB			DIB4501.8 blended with stellar lines	DIB 4501.8, 3.5%, 100mA	DIB 4501.8, 2.5%, 63mA
4590 CoronA					
4987 COHPyrB	DIB 4963.96, 4.5%, 31mA DIB 4969.67, 1.2%, 10mA DIB 4984.73, 3%, 13mA	Low S/N (here and above)	DIB 4963.96, 5.5%, 30mA DIB 4969.67, 2%, 30mA DIB 4984.73, 2%, 30mA	DIB 4963.96, 1.5%, 15mA DIB 4969.67, 1.3%, 10mA DIB 4984.73, 1%, 8mA	DIB 4963.96, 2%, 15mA DIB 4984.73, 1.5%, 3mA
5022 b(ghi)perA		New feature 5025, 7%, 2mA			
5251 PerylA					
6120 NaphtB2 (projected value)*	DIB 6116.65, 2.5%, 19mA	DIB 6116.65, 3.3%, 28mA		DIB 6116.65, 2%, 9mA	
6489 NaphtB1*		DIB 6491.88, 2.5%, 22mA	DIB 6491.88, 3%, 22mA	DIB 6491.88, 4.5%, 22mA	
6706 NaphtA*	DIB 6699.37, 4%, 23mA DIB 6701.98, 2.2%, 4mA	DIB 6699.37, 4.7%, 35mA DIB 6701.98, 3.5%, 10mA	DIB 6699.37, 3%, 15mA	DIB 6699.37, 2%, 19mA	DIB 6699.37, 3%, 20mA DIB 6701.98, 1%, 6.5mA
7229 perylB1		DIB 7249.26, 2.8%, 43mA DIB 7257.35, 1%, 15mA	DIB 7224.18, 19%, 200mA	DIB 7224.18, 15%, 200mA	DIB 7224.18, 8%, 125mA
7256 perylB2		DIB 7249.26, 2.8%, 43mA DIB 7257.35, 1%, 15mA DIB 7276.7, 6%, 33mA	DIB 7224.18, 19%, 200mA DIB 7276.7, 3%, 15mA	DIB 7224.18, 15%, 200mA DIB 7276.7, 2.5%, 20mA	DIB 7224.18, 8%, 125mA
7580 1MePyrB	DIB 7585.63. 1.8%, 30mA (Stellar CIII?)	DIB 7581.24, 5%, 39mA	DIB 7562.24, 6%, 100mA DIB ~7585 as one, 2%, 70mA DIB 7585.63, 1.5%, 30mA	DIB 7558.5, 1.5%, 26mA DIB 7562.24, 3%, 70mA DIB7579.17, 2%, 32mA DIB 7581.24, 2%, 29mA DIB 7585.63, 1%, 18mA	DIB7562.24, 3.5%, 30mA
7584 b(ghi)perB	see above	see above	see above	see above	see above
7588 4MePyrC	see above	see above	see above	see above	see above
8321 PentacB	DIB 8283.45, 1.5%, 44mA	DIB 8283.45, 5.3%, 55mA new feature DIB 8321, 6.3%, 44mA	DIB 8283.45, 3.5%, 60mA	DIB 8283.45, 3%, 31mA	
8566 PhenantB			DIB8566 blended with stellar lines, 1.5%, 120mA	DIB8530.79 is stellar line - HeI	
8648 TetracA	DIB 8621.23, 4.5%, 290mA	DIB 8621.23, 16.6%, 600mA	DIB 8621.23, 7%, 440mA	DIB 8621.23, 7%, 447mA	DIB 8621.23, 6.5%, 650mA
8839 1,2benzanthA					
8983 PhenantA					
9124 B(e)pyrB					
9310 MePhenA					
9433 PentacA					
9470 CoronB					
		DIB 9577, 10%, 380mA DIB 9632, 11%, 280mA	DIB 9577, 9%, 300mA DIB 9632, 7.5%, 215mA	DIB 9577, 5%, 200mA DIB9632 blended with MgII, 7%, 180mA	

Note: Tetrac: Tetracene, $C_{18}H_{12}^{+}$; B(e)pyr: Benzo(e)pyrene, $C_{20}H_{12}^{+}$; Pyrene: Pyrene, $C_{16}H_{10}^{+}$; 1MePyr: 1-Methylpyrene, $CH_3C_{16}H_9^{+}$; 4MePyr: 4-Methylpyrene, $CH_3C_{16}H_9^{+}$; COHPyr: 1-Pyrenealdehyde, 1MePyr: 1-Methylpyrene, $COHC_{16}H_9^{+}$; Coron: Coronene, $C_{24}H_{12}^{+}$; b(ghi)per: Benzo(ghi)perylene, $C_{22}H_{12}^{+}$; Peryl: Perylene, $C_{20}H_{12}^{+}$; Naphth: Naphthalene, $C_{10}H_8^{+}$; Pentac: Pentacene, $C_{22}H_{14}^{+}$; Phenant:: Phenanthrene, $C_{14}H_{10}^{+}$; 1,2benzanth: 1,2-benzanthracene, $C_{18}H_{12}^{+}$; MePhen: Methylphenanthrene, $CH_3C_{14}H_9^{+}$.
A = Strongest absorption band in the NUV - NIR range, B = second strongest band, and so forth; *Gas-phase data from CRDS measurements (Romanini et al, 1999).

Fig. 1.— Absorption spectra of the benzo(e)pyrene cation ($C_{20}H_{12}^+$; Top panel) and the benzo(ghi)perylene cation ($C_{22}H_{12}^+$; Bottom panel) isolated in neon matrices at 4.2 K.

Fig. 2.— Absorption spectra of the phenanthrene cation ($C_{14}H_{10}^+$; Top panel) and the pentacene cation ($C_{22}H_{14}^+$; Bottom panel) isolated in neon matrices at 4.2 K.

Fig. 3.— The spectral range around the carbohydroxypyrene ion ($(COH)C_{16}H_9^+$) feature near 4499 Å (Laboratory position from MIS experiments). Note the presence of the strong 4502 DIB in its close vicinity.

Fig. 4.— The spectral range around the naphtalene ion ($C_{10}H_8^+$) feature near 6706 Å (Laboratory position from *gas-phase* experiments of Romanini et al. (1999)). Note the presence of several weak and very weak DIBs in its close vicinity.

Fig. 5.— The spectral range around the naphtalene ion ($C_{10}H_8^+$) feature near 6489 Å (Laboratory position from *gas-phase* experiments of Romanini et al. (1999)).

Fig. 6.— Weak interstellar features in the spectra of heavily reddened stars close to the laboratory positions of the 1-methylpyrene ($CH_3C_{16}H_9^+$), benzo(ghi)perylene ($C_{22}H_{12}^+$) and 4- methylpyrene ($CH_3C_{16}H_9^+$) ions (Laboratory positions from MIS experiments).

Fig. 7.— The spectral range around the phenanthrene ($C_{14}H_{10}^+$) and the tetracene ($C_{18}H_{12}^+$) ion features near 8566 and 8648 Å respectively (Laboratory positions from MIS experiments). Note the presence of the strong 8621 DIB in the close vicinity of the tetracene ion absorption.

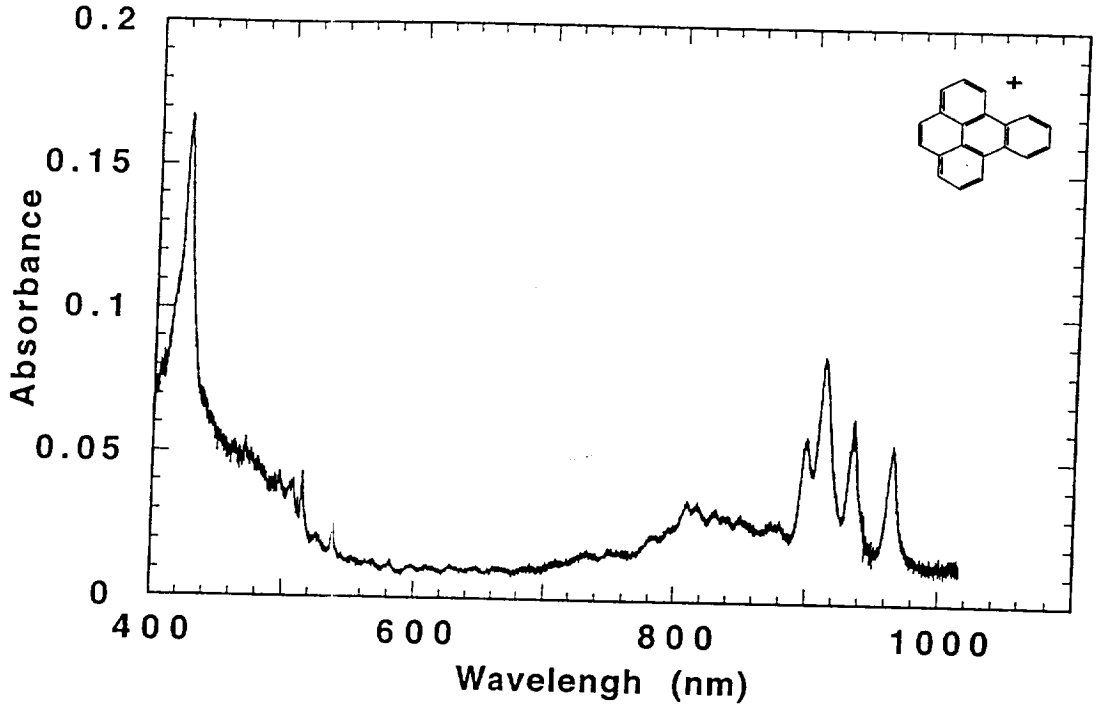
0.2
0.15
0.1
0.05
0
Absorbance
400
600
800
1000
Wavelengh (nm)
+

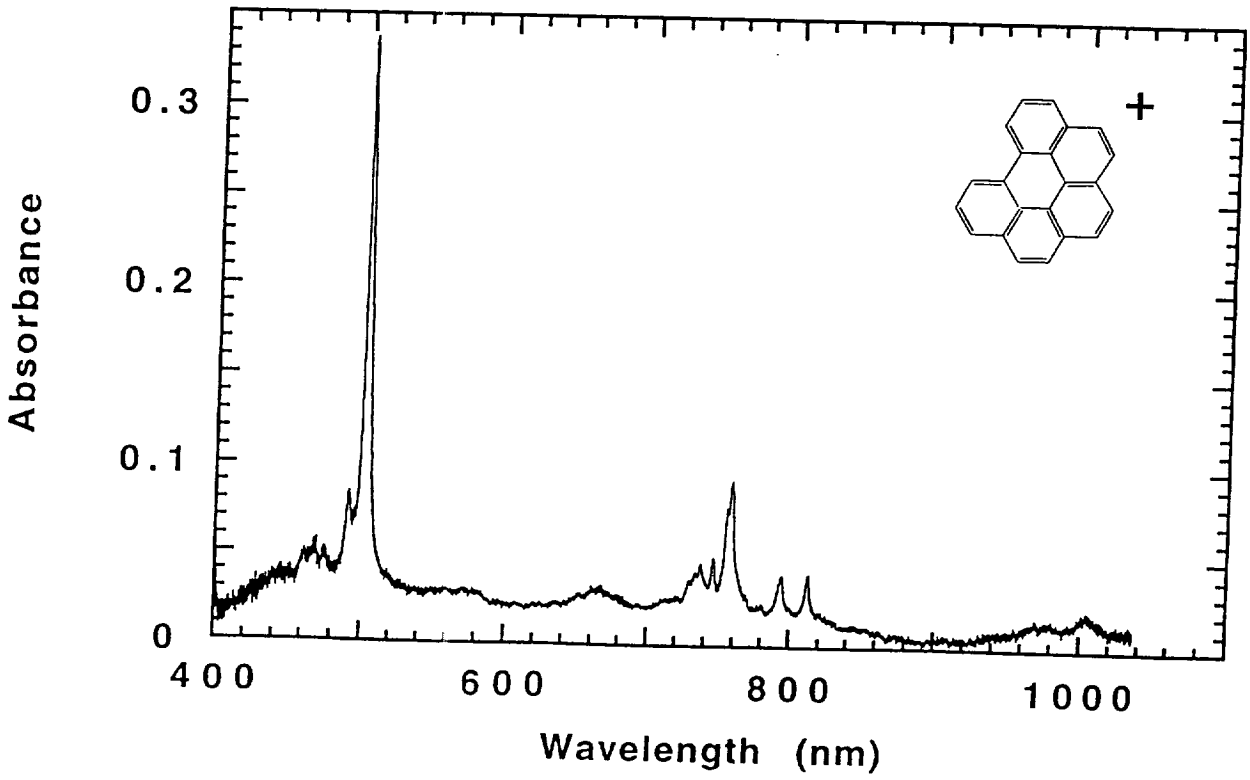
0.3
0.2
0.1
0
Absorbance
400
600
800
1000
Wavelength (nm)
+

Fig 1 /Suite

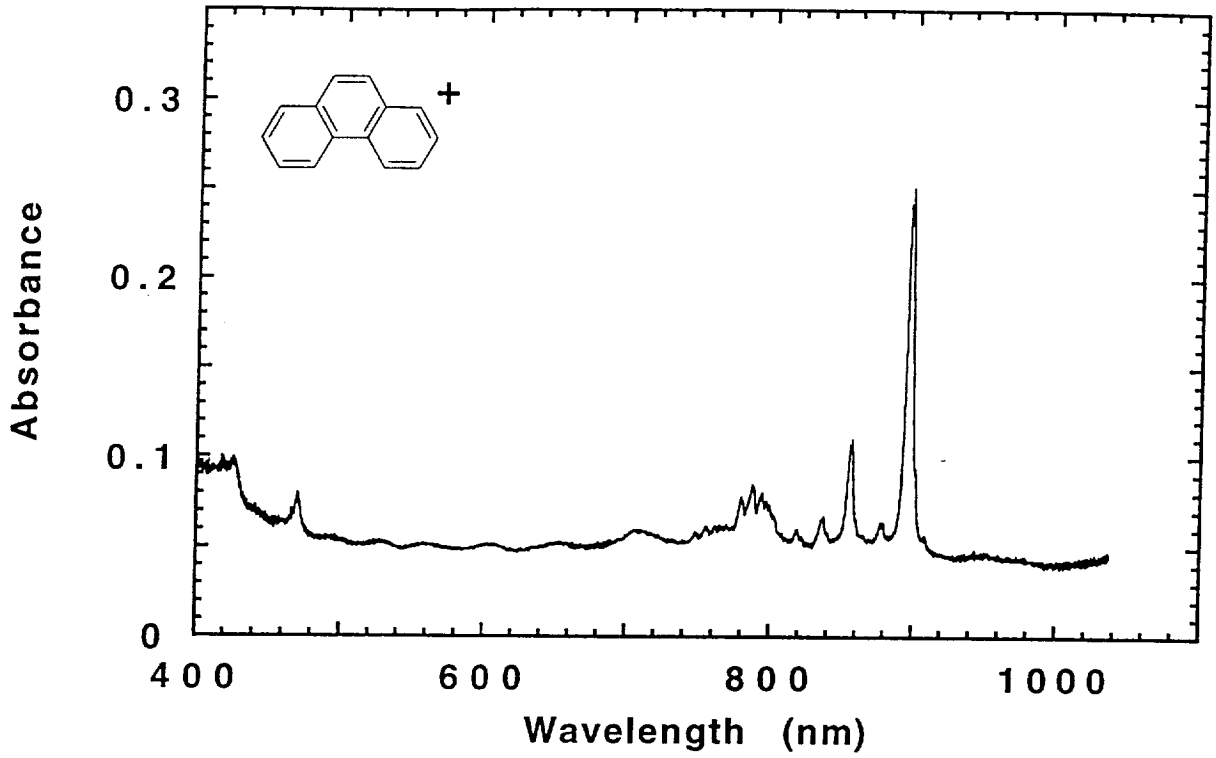
0.3
0.2
0.1
0
Absorbance
400
600
800
1000
Wavelength (nm)
+

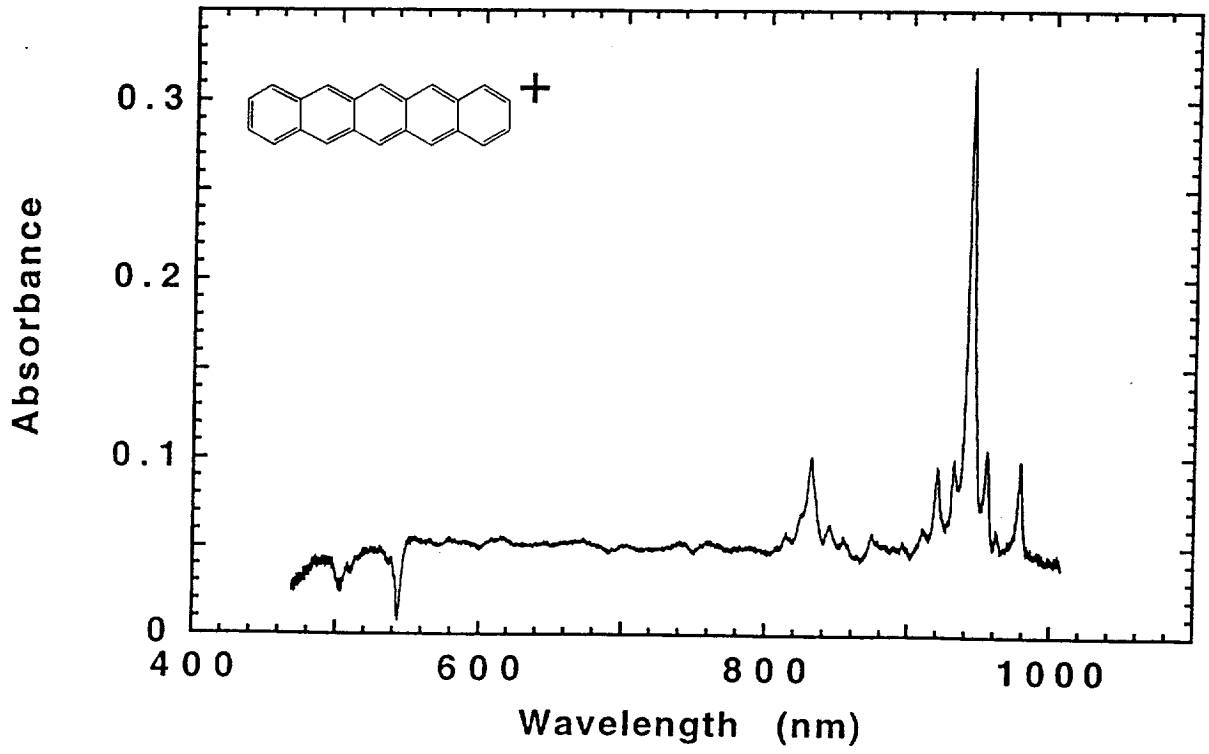
0.3
0.2
0.1
0
Absorbance
400
600
800
1000
Wavelength (nm)
+

Fig. 2 / Palmer

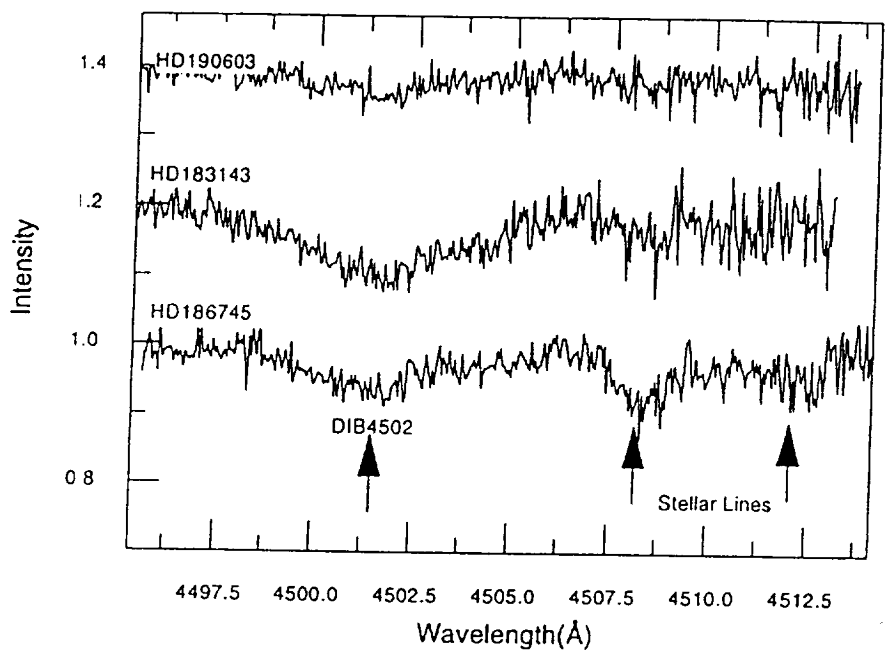

Fig. 3/ Sakaura

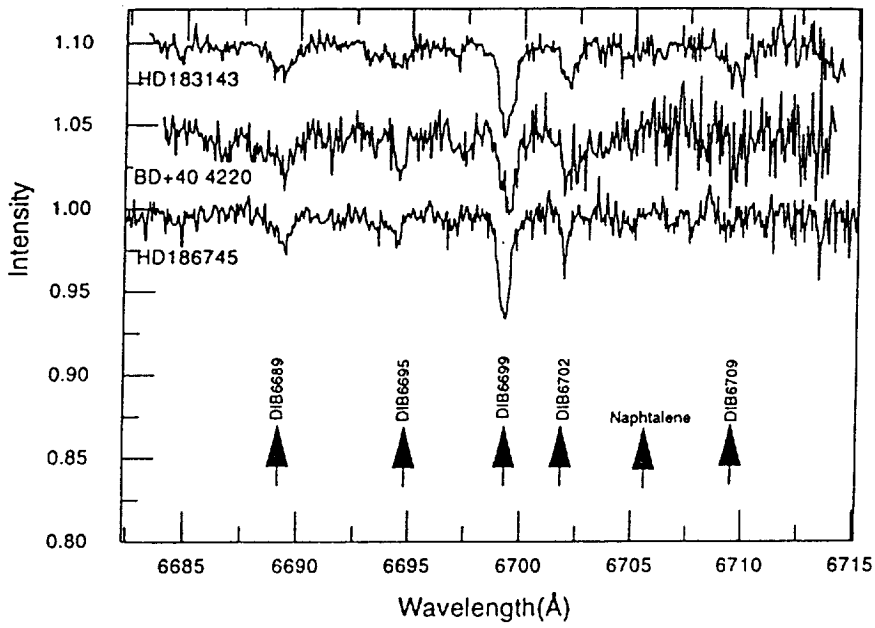
1.10
1.05
1.00
0.95
0.90
0.85
0.80
Intensity
HD183143
BD+40 4220
HD186745
DIB6689
DIB6695
DIB6699
DIB6702
Naphtalene
DIB6709
6685
6690
6695
6700
6705
6710
6715
Wavelength(Å)

Fig. 4 Salama

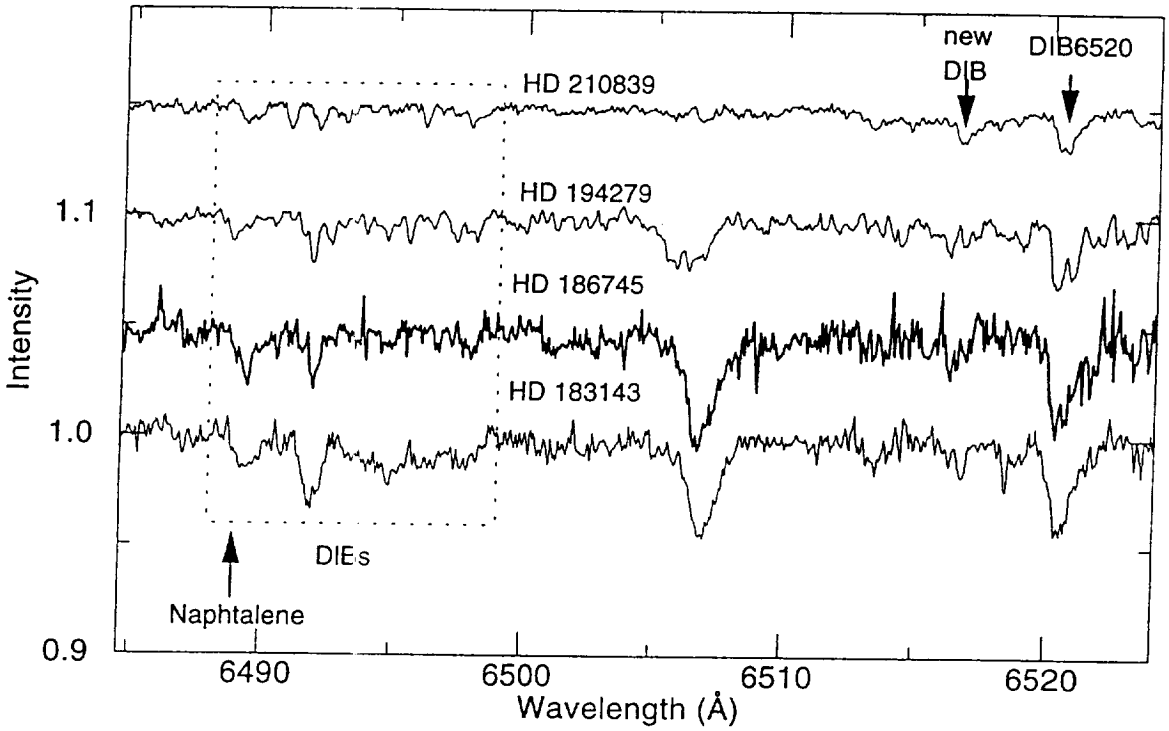
new
DIB
DIB6520
HD 210839
HD 194279
HD 186745
HD 183143
DIEs
Naphtalene
Intensity
1.1
1.0
0.9
6490
6500
6510
6520
Wavelength (Å)

Fig. 5 / Salama

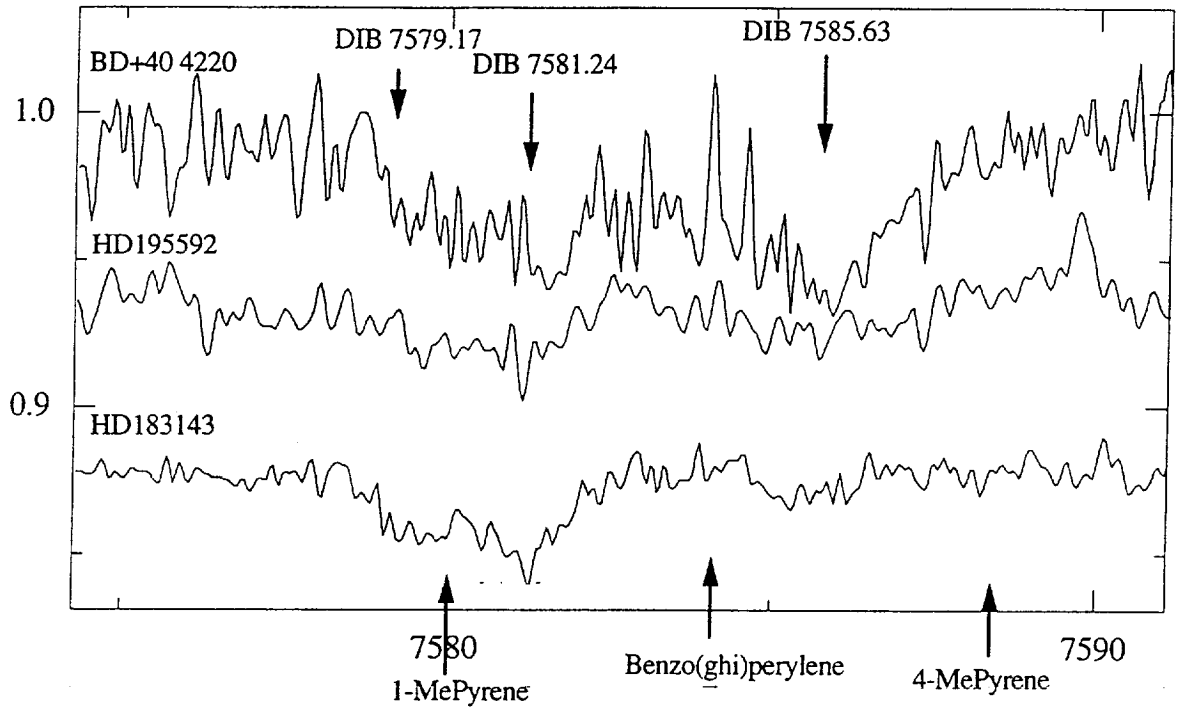
DIB 7579.17
DIB 7581.24
DIB 7585.63
BD+40 4220
HD195592
HD183143
1.0
0.9
7580
7590
1-MePyrene
Benzo(ghi)perylene
4-MePyrene

Fig. 6 Salama

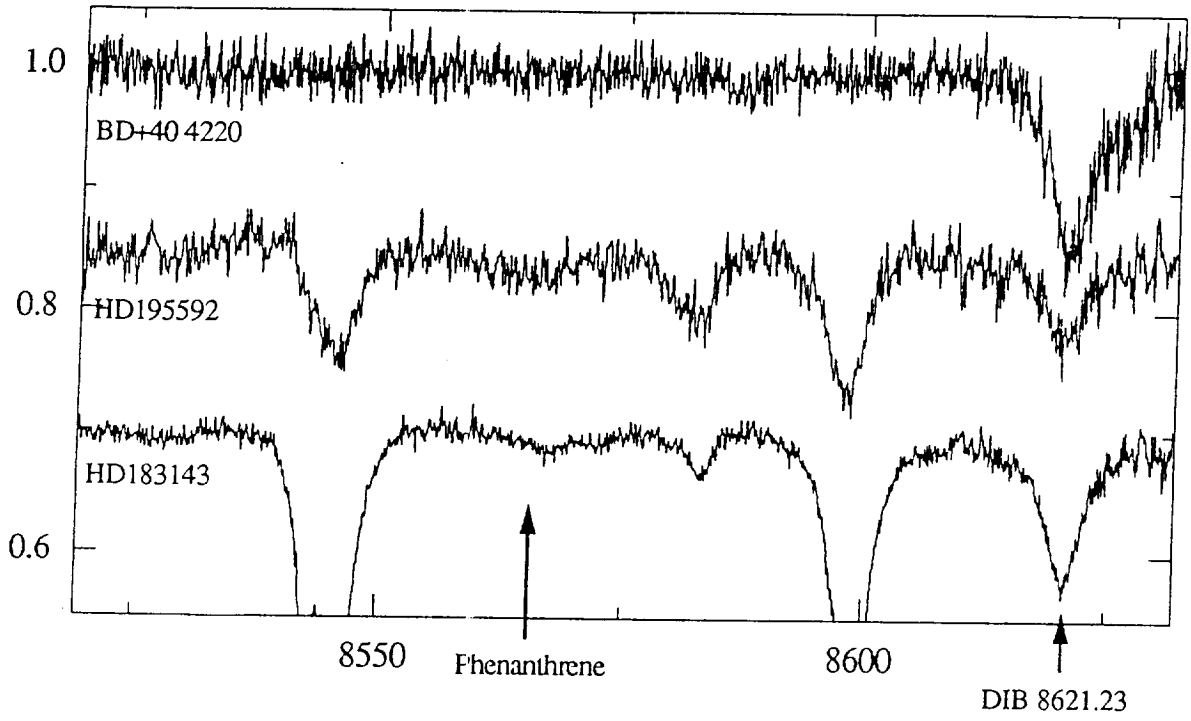
1.0
BD+40 4220
0.8
HD195592
HD183143
0.6
8550
Phenanthrene
8600
DIB 8621.23

Fig. 7 / Salama